

Impact of Calcium on Inhibition Mechanism and Performance of Two Polymer-Based Silicate Scale Inhibitors in Low Enthalpy Geothermal Brine Systems

Shabnam Mohammadi^{1*}, Kenneth Stuart Sorbie¹, Lorraine Scott Boak¹, Eric James Mackay^{1,2}, Khosro Jarrahan²

¹Heriot-Watt University, Edinburgh, EH14 4AS, UK

²Petronas Centre of Excellence in Subsurface Engineering and Energy Transition (PACESSET), Heriot-Watt University Edinburgh, EH14 4AS, UK

*sm2219@hw.ac.uk

Keywords: Silicate Scale, Scale Inhibitor, Inhibition Efficiency and Mechanism, Low Temperature, Geothermal Brine Systems

ABSTRACT

Silica scaling is an operational issue in geothermal energy production. In this work, a static bottle test methodology was developed to assist in identification of silicate inhibitors, demonstrating 80-90% inhibition performance, for application in low-enthalpy geothermal systems. To identify effective products for the control of amorphous and magnesium silicate scaling, the inhibition mechanisms and inhibition efficiency (IE) of two sulphonated polymer-based scale inhibitors, denoted A5 and SI B, were studied. This was performed for a brine containing $[Mg]_{\text{initial}} = 120\text{ppm}$ and $[Si]_{\text{initial}} = 1880\text{ppm}$ at 95°C and pH8.5. The impact of adding 500ppm_{mix} calcium was subsequently assessed.

In the absence of calcium, a minimum inhibitor concentration (MIC) of ~50ppm for SI B and ~100ppm for A5 were required to control amorphous and magnesium silicate scale effectively at ~60-90% IE. In the system containing calcium, although two approaches were used to adjust the pH of the brine to 8.5, to reduce the tendency for $\text{Ca}(\text{OH})_2$ precipitation, and thereby improve scale inhibitor effectiveness, it was found that neither SI B nor A5 prevented precipitation of silicate-based scale.

To identify the inhibition mechanisms, two complementary methods were compared to track SI consumption. The first measured sulphur content, unique to the structure of SI B and A5, using Inductively Coupled Plasma Optical Emission Spectrometry (ICP-OES). The second employed a matrix-matching Hyamine technique, targeting the functional groups along the polymer backbone to detect the inhibitor directly.

1. INTRODUCTION

In recent years, global energy demand has risen significantly, driven by rapid population growth and expanding industrial activity. While fossil fuels currently supply much of this demand, growing awareness of their environmental impacts has highlighted the urgent need for cleaner, renewable alternatives, such as geothermal, solar, wind, and hydro energy (Li et al., 2023; Shah et al., 2024). Among these renewable alternatives, geothermal energy is a cost-effective and technically proven one, which offers a promising path toward a cleaner and more resilient future (Solano-Olivares et al., 2024). Its remarkable potential as a sustainable energy source has captivated researchers and industry professionals. Sustainability, weather independence, stability, operational reliability, and

environmentally friendly characteristics distinguish this energy source from other clean sources (Hassani & Zheng, 2024; Ouerghi et al., 2024).

Despite its many advantages, geothermal energy faces a significant challenge: scaling. A geothermal brine is a complex mixture of dissolved minerals and gases, and at high temperatures, it can lead to the formation of mineral deposits, commonly referred to as scaling. Scaling occurs when the concentration of certain salts exceeds their equilibrium solubility, causing them to precipitate. This process is driven by changes in Gibbs free energy, which leads to a supersaturated solution moving towards equilibrium through the formation of solid phases. Scaling can severely impact operations, leading to the plugging of wells and pipelines, and ultimately causing production curtailments in geothermal power plants (Hassani & Zheng, 2025; Isik et al., 2023).

Calcium carbonate, calcium silicate, magnesium silicate and amorphous silica scale are the major constituents in geothermal fluids, while calcium sulphate, barium sulphate, calcium oxalate, strontium sulphate, and colloidal iron oxides are seen in some sites (Finster et al., 2015; Heřmanská et al., 2019). Silica scaling is a problem that can occur in medium and high enthalpy geothermal fields. In hydrothermal fields, silica occurs in different forms at different depths. These are generally in the form of amorphous silica, chalcedony, cristobalite, and quartz. Quartz is the most stable form of silica with the lowest solubility among these forms. The solubility of amorphous silica in geothermal waters decreases with temperature and creates a scale problem in regions where steam separation and cooling occur. Therefore, transmission lines, heat exchangers, reinjection wells, and in some cases, production wells in geothermal power plants are the riskiest equipment in terms of amorphous silica scaling (Pambudi, 2015; Petkowski et al., 2020).

In geothermal systems, the change in temperature and pH are the most notable parameters that affect their scaling systems (Jarrahian et al., 2025). Generally, brines with a low and moderate temperature (<150°C) end up with the formation of calcium carbonate whilst high-temperature ones with high Total Dissolved Solid (TDS) content yield siliceous scales (Buscarlet et al., 2016; Khasani et al., 2021). An increase in system pH causes major cations in geothermal fluids such as Fe^{2+} , Mg^{2+} , and Ca^{2+} to precipitate as hydroxides. Additionally, elevated pH levels, combined with the presence of these metal ions, promote silica polymerization. Metal hydroxides can interact with polymerized silica to form metal silicate compounds, which are highly insoluble and difficult to remove. These compounds typically exist in amorphous, oligomeric forms, resembling colloidal silica in structure (Gören et al., 2021).

There is an increased need to understand the scaling system and to mitigate it. Generally, the elimination of silica deposition before it is formed is one of the frequently used methods. However, silica polymerization has not been completely understood yet because every geothermal fluid has unique characteristics due to different environmental conditions such as salinity, temperature, and water-rock interactions. Installation of an inhibitor system is the most effective and practical solution to prevent scaling problems and production loss, if the optimum inhibitor dosages are determined and applied effectively in geothermal systems. There are a wide variety of inhibitor products available on the market, however selection is dependent on the problems encountered. Scale inhibitor application is carried out to prevent the calcite, silica, stibnite, and other possible scale formations, and they are picked up according to the reservoir temperatures of geothermal wells (Morita et al., 2021; Mpelwa & Tang, 2019; Olajire, 2015).

From a performance standpoint, if scale inhibitors could function as nucleation inhibitors, these prevent the formation of scaling minerals by forming water-soluble complexes with specific ions in the brine. These inhibitors are particularly effective against colloidal particles by interfering with both homogeneous and heterogeneous nucleation processes. In contrast, crystal growth inhibitors work by adsorbing onto the surface of growing crystals and binding on active growth sites. This interaction hinders crystal development, distorts crystal morphology, and ultimately reduces crystal stability (Abib et al., 2018; Anderson et al., 2011; Scott et al., 2024).

From the perspective of chemical structure and functional mechanism, scale inhibitors are primarily classified into two main types: phosphonates and polymers (Khormali et al., 2023; Liu et al., 2022; Shi et al., 2022). Polymer type inhibitors are generally preferred when the reservoir temperature exceeds 210°C, as these inhibitors demonstrate greater stability at higher temperatures in geothermal reservoirs (Haklidir & Haklidir, 2017). Various polymeric macromolecules have been used as silicate-based scale inhibitors in geothermal systems, and commercially, there is a wide range of scale inhibitors in the market (Çiftçi et al., 2020; Gill, 2011). However, the vital point is to test and choose the most applicable one for the field according to the physical conditions (pH, temperature, pressure, etc.) and chemical composition of the field. Research shows that a suitable inhibitor to inhibit the silica-based deposit, especially colloidal silica and magnesium silicate and any other scale that acts as a nuclei, in silicate precipitation, such as calcium carbonate and calcium sulfate, are polymer species with M.Wt.< 10,000 Da and contain carboxylic acid and sulfonic acid groups (Amjad & Zuhl, 2010; Matorian & Malaieri, 2022).

As the synthesis of artificial geothermal deposits in the laboratory, under specific conditions, is a more practical and economical way to perform scale inhibitor performance tests, in this work, a static bottle test methodology was developed to assist in identification of efficient silicate inhibitors (IE% ~80-90%), applicable in low-enthalpy geothermal systems. To identify effective products for the control of silicate scaling, the inhibition mechanisms and inhibition efficiency (IE) of two sulphonated polymer-based scale inhibitors, denoted A5 and SI B, were studied. This was performed for a brine containing $[Mg]_{\text{initial}} = 120\text{ppm}$ and $[Si]_{\text{initial}} = 1880\text{ppm}$ at 95°C, pH8.5 and their active concentration range 20-200ppm. Further research examined the inhibition performance and mechanism of scale inhibitor B and A5 in the presence of $[Ca]_{\text{mix}} = 500\text{ppm}$ at 95°C and pH8.5. To evaluate the inhibition mechanism, two methods were compared, one measuring the concentration of sulphur (S) by ICP-OES, and two, using a matrix-matching Hyamine technique, to enable A5 and SI B to be assayed as a polymer product.

For the silicate system of 60ppm Mg and 940ppm Si, MIC of ~50ppm for SI B and ~100ppm for A5 were required to control amorphous and magnesium silicate scale effectively at ~60-90% IE. Although two different approaches were employed to adjust the pH of the brine in the system containing 500 ppm calcium, with the aim of reducing $\text{Ca}(\text{OH})_2$ precipitation and enhancing scale inhibitor performance, both SIs failed to prevent the formation of silicate-based scale.

2. EXPERIMENTAL METHODS

2.1 Material

Silicon brine (SB) containing 1880ppm of silicon ion (Si^{4+}) was prepared by dissolving 14.2 grams of sodium metasilicate pentahydrate ($\text{Na}_2\text{SiO}_3 \cdot 5\text{H}_2\text{O}$) (Sigma Aldrich, $\geq 95.0\%$ (T)) in 1L of distilled water (DW). The magnesium brine (MB) was prepared by adding 1.003 grams of magnesium chloride

hexahydrate salt ($\text{MgCl}_2 \cdot 6\text{H}_2\text{O}$) (Merck) in 1L of DW to produce an initial concentration of 120ppm magnesium ions (Mg^{2+}). A 1L brine containing 120ppm magnesium ion (Mg^{2+}) and 1000ppm of calcium ion (Ca^{2+}) was prepared by dissolving 1.003 grams of magnesium chloride hexahydrate salt ($\text{MgCl}_2 \cdot 6\text{H}_2\text{O}$) and 5.466 grams of calcium chloride hexahydrate salt ($\text{CaCl}_2 \cdot 6\text{H}_2\text{O}$) (Merck) in DW. The prepared brine solutions were filtered using 0.45 μm filter paper. A quenching solution of 1% EDTA/NaOH was prepared by mixing 10g of EDTA (Ethylene diamine tetra acetic acid disodium salt dihydrate) (VWR) with 10g sodium hydroxide (VWR) and the solution was made up to 1L using distilled water. In addition to MB, SB, Mg:Ca brine and quench solution, the scale inhibitor (SI) A5 and SI B stock solutions (10,000ppm active) were prepared in 250ml magnesium brine and 250ml Mg:Ca brine by adding 5.56 and 12.5 grams of A5 and SI B, respectively. A5 is a low molecular weight and water-soluble polymer that contains 2-acrylamido-2-methylpropane sulfonic acid (AMPS/ATBS), acrylic, maleic and another non-ionic monomer (but not the allyloxy benzene sulfonate monomer). SI B is a sulphonated acrylic co-polymer with molecular weight of ~ 7200 .

2.2 Inhibition Efficiency Test Procedure

SI stock solutions were diluted further in MB or Mg:Ca brine to generate the x2 higher concentrated solutions initially required to allow for the final [SI] in the 50:50 mixed brine. Once generated, these 300ml individual MB or Mg:Ca brine including SI solutions, were added to their respective 300ml SB and shaken vigorously. Their pH was adjusted to the required pH8.5 using 10% HCl. For the system containing Ca ion, another pH adjusting approach was also taken with the assumption of suppressing $\text{Ca}(\text{OH})_2$ precipitation at the high initial mixing pH of ≥ 12 and boosting the scale inhibitors efficiency. SB pH was initially adjusted to 8.5 before mixing it with Mg:Ca brine including SI. Then, after mixing the brines, pH was adjusted again to 8.5. At this stage, the large 600ml volume of pH-adjusted mixed brine was split into 6x100ml aliquots into 250ml labelled HDPE bottles. At each sampling time interval, the sample bottles were removed from the oven, a 10ml sample withdrawn via a syringe was filtered using a 0.2 μm nylon filter and collected in a labelled test tube. A volume of this filtered sample was diluted appropriately in 1% EDTA/NaOH solution and analysed for Si, Mg, Ca and S ions by ICP-OES. For the Mg, Si and Ca analysis, it was a x10 dilution - 1ml of the filtered tests was pipetted into labelled test tubes including 9ml of 1% EDTA/NaOH. For the S analysis, it was a x2 dilution - 5ml of the remaining filtered tests was pipetted into labelled test tubes containing 5ml of 1% EDTA/NaOH. In addition, various filtered sample volumes up to 5ml were used/diluted for Hyamine analysis. This static bottle test procedure is shown in Fig. 1 schematically.

2.3 ICP-OES Spectroscopy

These tests used an “ion reacted” approach (see below) so that the individual changes in magnesium, silicon and calcium concentrations are measured by ICP-OES.

$$\text{X ion reacted (ppm)} = [\text{X}]_0 - [\text{X}]_f \quad (1)$$

Where $[\text{X}]_0$ and $[\text{X}]_f$ are the initial and final values of X where X = magnesium, silicon and calcium ions concentration, respectively.

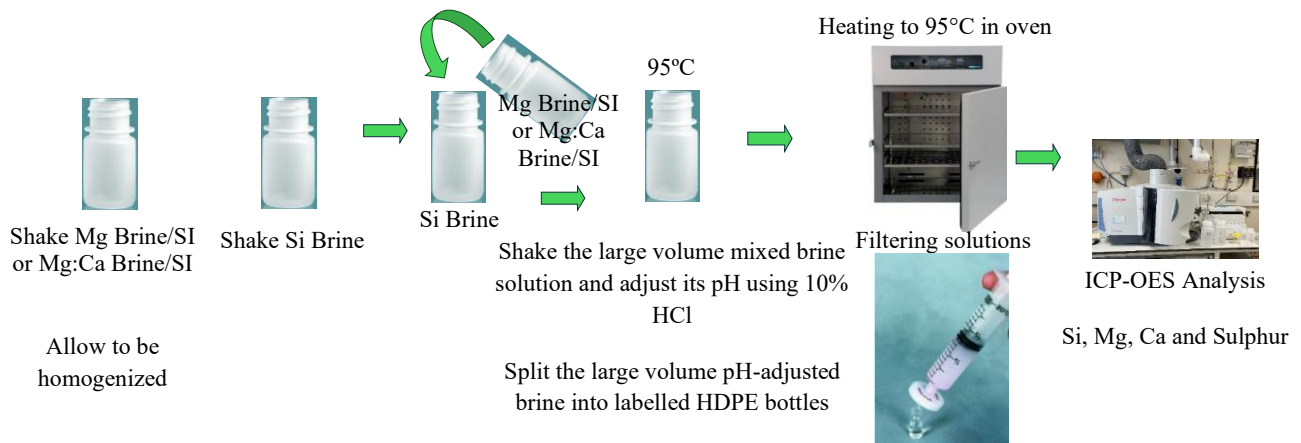


Fig. 1: Brine mixing and pH adjustment procedure for silicate scale inhibition efficiency test and scale inhibitor consumption by ICP-OES.

In fact, it is the remaining concentrations in solution after any silicate precipitation has occurred that is measured by ICP-OES however it is convenient to plot the amount of Mg, Si or Ca which has reacted i.e. the amount missing from solution that is in the precipitate.

$$X \text{ ion reacted } \% = (X \text{ ion reacted (ppm)})/[X]_0 \times 100 \quad (2)$$

The inhibition efficiency of SI to inhibit the silicate scaling was calculated using Equation 3.

$$\% \text{ Efficiency } (t) = \frac{(C_I - C_B) \times 100}{(C_0 - C_B)} \quad (3)$$

C_0 = Concentration of silicon (or other cations) originally in solution (i.e. $t=0$).

C_I = Concentration of silicon (or other cations) at sampling.

C_B = Concentration of silicon (or other cations) in the blank solution (no inhibitor).

(t) = Sampling time.

$IE_{Mg} \%$, $IE_{Si} \%$ and $IE_{Ca} \%$ are the inhibition efficiency percentages calculated using magnesium as the scaling ion using, silicon as the scaling ion and calcium as the scaling ion, respectively.

For sulphur consumption, at each scale inhibitor concentration, the sulphur concentration in solution after any silicate precipitation is measured by ICP-OES. Then, the contribution of scale inhibitor in the inhibition procedure is specified by calculating the amount of consumed sulphur using this formula:

$$\text{Sulphur Consumed (ppm)} = [S]_{\text{Control Solution}} - [S]_{\text{ICP}} \quad (4)$$

Where $[S]_{\text{Control Solution}}$ and $[S]_{\text{ICP}}$ are the Sulphur concentrations in control solution and measured value by ICP-OES, respectively.

Here is the formula to calculate percentage of consumed Sulphur:

$$\text{Sulphur Consumed } \% = (1 - ([S]_{\text{ICP}} / [S]_{\text{Control Solution}})) \times 100 \quad (5)$$

2.4 Matrixed Matched Hyamine Procedure

For the Hyamine analysis, initial inhibitor stock solutions (1000ppm) were prepared in their appropriate matrices. The SI stocks/samples were then diluted down to 100ppm. From the 100ppm solutions, considering the dilution factors, 5ml standards, in test-tubes, were prepared as well as at repeat concentrations, 0, 2, 5 and 8 ppm. Depending on the dilution factor for each sample concentration (x2 for blank and 20ppm, x10 for 50ppm, x20 for 100ppm and x40 for 200ppm), the required volume was taken out of the remaining 10ml filtered test solution (6ml of the filtered test solution was already used for Si, Mg, Ca and sulphur ions analysis by ICP-OES) and pipetted into an appropriate volume of 1% EDTA/NaOH to prepare 5ml solutions at the appropriate dilution factor. Then, 1ml of 5% sodium citrate and 1ml of 0.5% Hyamine 1622 solution was added to each standard, control and test solution. A time interval of 1 minute for the addition of sodium citrate and Hyamine to the next test-tube was given. The samples were then left for 40 minutes. After 40 minutes, at their 1minute intervals, the absorbance values were measured. The recorded test solution absorbance values were then inputted into the appropriate previously constructed matrix matched calibration graph to determine their scale inhibitor concentrations. Fig.2 explains this procedure schematically.

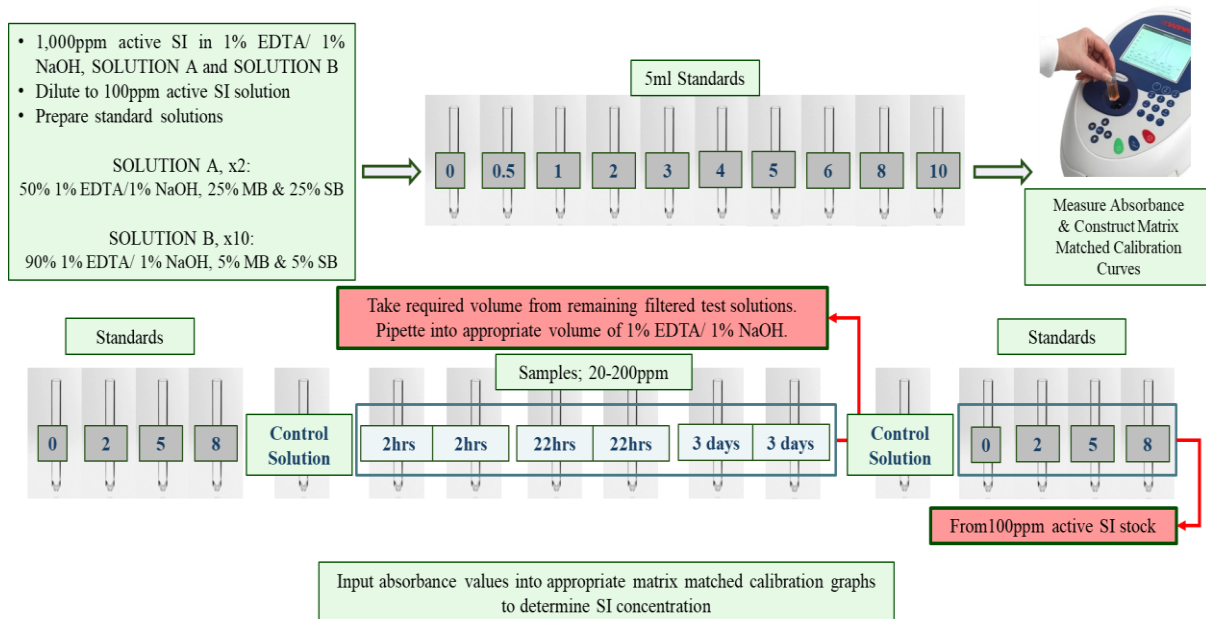


Fig. 2: Procedure for scale inhibitor consumption by matrix matched Hyamine technique.

3. RESULTS AND DISCUSSIONS

3.1 SI B Inhibition Efficiency and Mechanism for Silicate System of 60Mg:940Si at 95°C and pH8.5, 20-200ppm SI B Active Concentration

The ions reacted (%) were plotted in Fig. 3. The results indicate that SI B exhibits an inhibitory effect, as a lower amount of Si and Mg ions reacted when ≥ 50 ppm of SI B was present. Over a 3-day reaction period, at SI B concentrations of ≥ 50 ppm, less than 20% of the Si and Mg ions reacted. In contrast, non-inhibited samples showed a significantly higher reactivity, with ~ 80 -100% of the ions reacting consistently across all time intervals.

Fig. 4 shows Mg and Si inhibition efficiencies. 50-200ppm SI B demonstrates good Si IE % at all time intervals of 2hrs, 22hrs and 3 days with 80-90% Si IE. Hence, 50-200ppm SI B was effective at inhibiting amorphous silicate scale. The lower 20ppm SI B concentration showed performance only at 2hrs although it was ~80% IE. The Mg IE showed a similar pattern to the Si IE at all time intervals and all SI B concentrations tested. [SI B] >50ppm, showed ~80-90% IE for all residence times with 20ppm managing 82% IE, only at 2hrs, and no IE for other residence times.

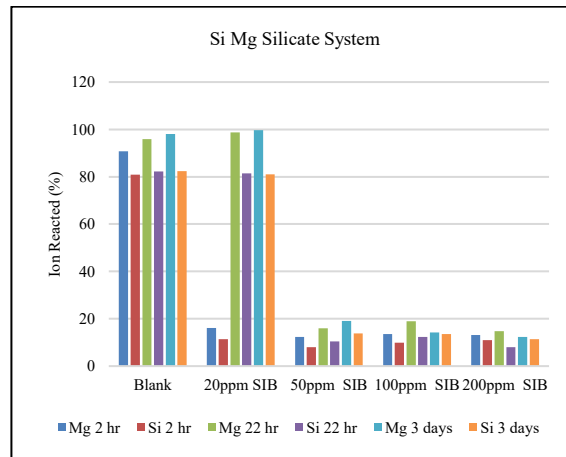


Fig. 3: Ions reacted (%) for 60Mg:940Si at 95°C, pH8.5 and 20-200ppm SI B.

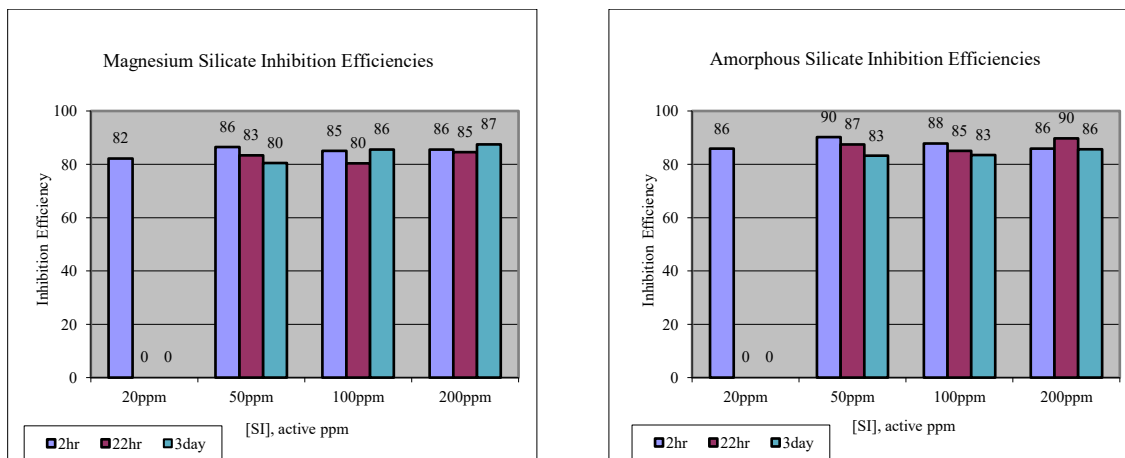


Fig. 4: Si and Mg IE% for 60Mg:940Si at 95°C, pH8.5 and 20-200ppm SI B.

The SI B remaining in solution (%) and Mg and Si IE % are shown in Fig. 5. For SI B concentrations ≥ 50 ppm, there was very little SI B sulphur consumption (less than 10%) over 3 days reaction time. Results obtained from the Hyamine method confirm this observation. The most significant reduction in polymer level in solution related to 20ppm SI B. This was ~80% decline, over 3 days reaction time. This corresponded to 20ppm SI B being able to only maintain inhibition efficiency performance up to 2hrs. At ≥ 50 ppm, the polymer consumption followed a similar pattern and fluctuated between 40% and 60% polymer remaining in solution after 2hrs. The differences between these two analytical methods, used to determine the scale inhibitor consumption profiles, indicated a more detailed investigation was required. The further investigation showed that the decline in SI inhibitor concentrations was more accurate and precise using the Hyamine analysis, as this was assaying a larger

proportion of functional groups attached to the polymer product. In comparison, the intensity of the sulphur signals via ICP-OES analysis, although accurate and precise, were not significant enough to determine the very small changes in sulphur concentration that were occurring for the higher SI concentrations ($\geq 50\text{ppm}$) when they were being less consumed in the inhibition process.

The inhibition efficiency and consumption results are evidence that at $\geq 50\text{ppm}$ the SI B operates initially through assisting in the dispersion of crystal embryos. Once crystallization has occurred, the inhibitor becomes very effective at retarding crystal growth (Graham et al., 2003).

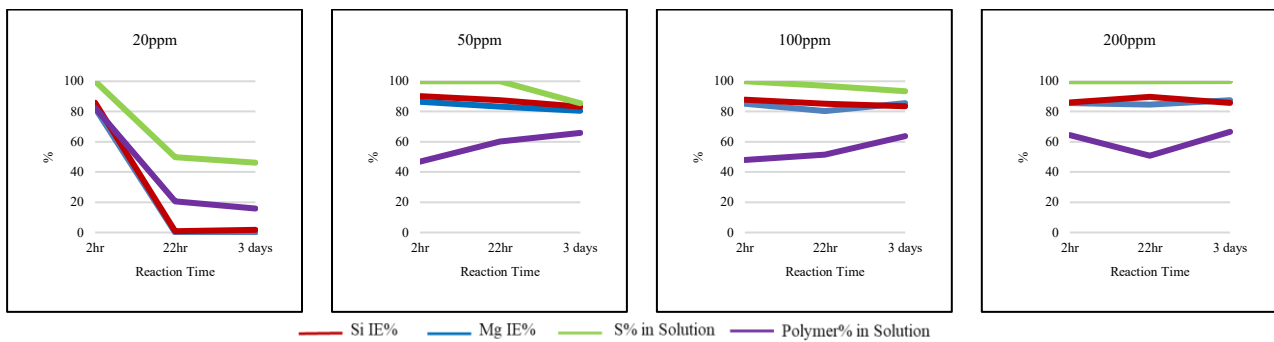


Fig. 5: SI B IE%, Sulphur and Polymer Consumption for 60Mg:940Si at 95°C, pH8.5 and 20-200ppm SI B.

3.2 SI B Inhibition Efficiency and Mechanism for Silicate System of 60Mg:940Si:500ppmCa at 95°C and pH8.5, 20-200ppm SI B Active Concentration

As previously explained, two distinct approaches were employed to perform the SI B inhibition efficiency test for the silicate system of 60Mg:940Si:500Ca at 95°C and pH8.5. It was believed that by preventing $\text{Ca}(\text{OH})_2$ precipitation that typically occurs at high pH, the efficiency of SI B in this system is affected positively. Fig. 6 presents the percentage of Si, Mg and Ca ions that reacted. When the pH of the mixed brine was adjusted to 8.5, for the non-inhibited solution, $\sim 20\%$ of the Ca ions reacted across all time intervals. However, the magnesium ion reacted, experienced a slight increase over time from 80% at 2hrs to more than 90% by 3 days reaction time. For the silicon ion reacted, the values remained almost constant over time at $\sim 80\%$. Hence, greater ions reacted was observed for Mg when compared with Ca. This indicates silicates favour Mg ions when both Ca and Mg ions are present in a non-inhibiting solution. The silica backbone has a higher tendency to bridge with Mg than Ca which agrees with that reported, where commonly encountered cations affect solubility, in the order of $\text{Mg} > \text{Ca} > \text{Sr} > \text{Li} > \text{Na} > \text{K}$ (Hauksson et al., 1995).

The addition of SI B resulted in less than a 5% decrease in the value of Ca ions reacted. Even at concentrations as high as 200ppm, SI B did not significantly impact the reaction of Ca ions. For the magnesium ions, the percentage of ions that reacted increased from 80% to over 95% by 22hrs and remained at this level to 3 days, in the solutions containing 20-200ppm SI B. The reaction of Si ions remained steady at around 80% over time, across all inhibiting samples. These observed trends are like those recorded for the blank solution. The results clearly indicate that the addition of SI B to the system did not effectively control scale precipitation, and increasing its concentration provided no observable improvement.

On the other hand, Fig. 6 shows the ions reacted percentage for the 60Mg:940Si:500Ca silicate system when pH of silicon brine was adjusted initially to 8.5 before mixing the brine. The most significant

change relates to the Mg ions reacted percentages. There was a drop of ~30% in the reacted Mg ions level at all time intervals for all sample solutions. However, Mg did keep its increasing trend over time from 2hrs to 3 days, as 50 to 80%, respectively. In addition to Mg, the Ca ions showed less reaction (by ~10% for some). However, the amount of reacted Si ions was not affected by the change in method for the brine pH-adjusting and its level remained at ~80% at all sampling times for non-inhibited and inhibited solutions.

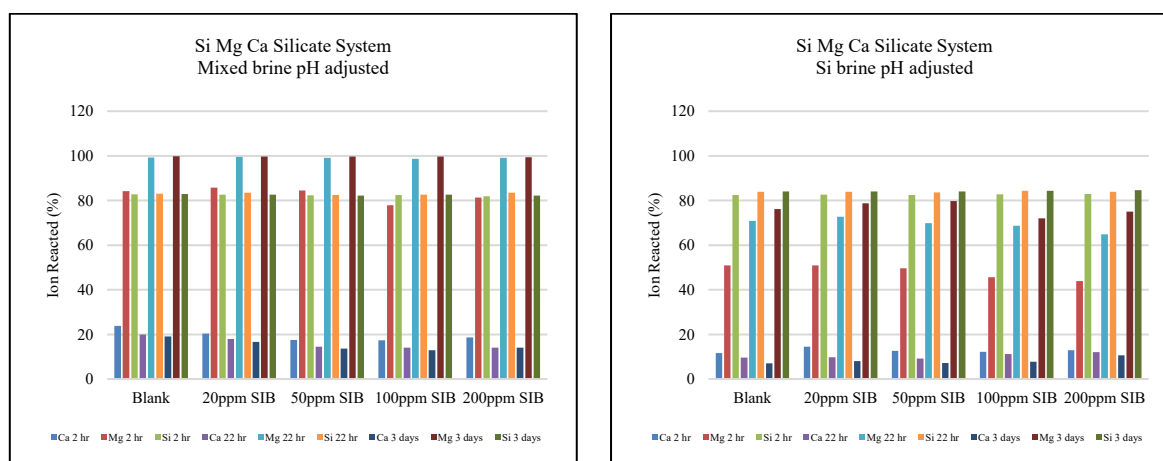


Fig. 6: Ion Reacted (%) for 60Mg:940Si:500Ca at 95°C, pH8.5 and 20-200ppm SI B, Mixed Brine pH Adjusted vs. Silicon Brine pH Adjusted.

The Si, Ca and Mg inhibition efficiencies at 2hrs, 22hrs and 3 days are shown in Fig. 7. It was observed that SI B is fully ineffective at preventing silicate-based scales even at its highest tested concentration of 200ppm. It appears the presence of 500ppm Ca ion in the silicate system of 60ppm Mg:940ppm Si makes the SI B inefficient at controlling calcium silicate, amorphous and magnesium silicate scale. Whilst in the absence of the Ca ion, as explained earlier, ~50ppm SI B was able to prevent amorphous and magnesium silicate scale. It seems that the effort to enhance the SI B inhibition performance through adjusting the pH of silicon brine before mixing the brines with the aim of avoiding $\text{Ca}(\text{OH})_2$ precipitation did not work. Although, this approach decreased the amount of Ca and Mg ions reacted to some extent, showing that perhaps $\text{Ca}(\text{OH})_2$ is formed under the mixed brine pH adjustment conditions.

The inefficient performance of SI B is shadowed by significant reductions in polymer levels recorded at the different SI B concentrations (Fig. 7). It showed a complete depletion over time. The values detected by Hyamine were approximately zero after 3 days. This trend was observed for both adopted approaches; mixed brine and silicon brine pH adjusted. This may be attributed to the entrapment of SI B within the scale structure, where it becomes incorporated into the scale matrix without effectively blocking active growth sites on the crystal surface. Although SI B is consumed during the process, it is ultimately immobilized within the scale and fails to inhibit the precipitation of silicate-based scale effectively.

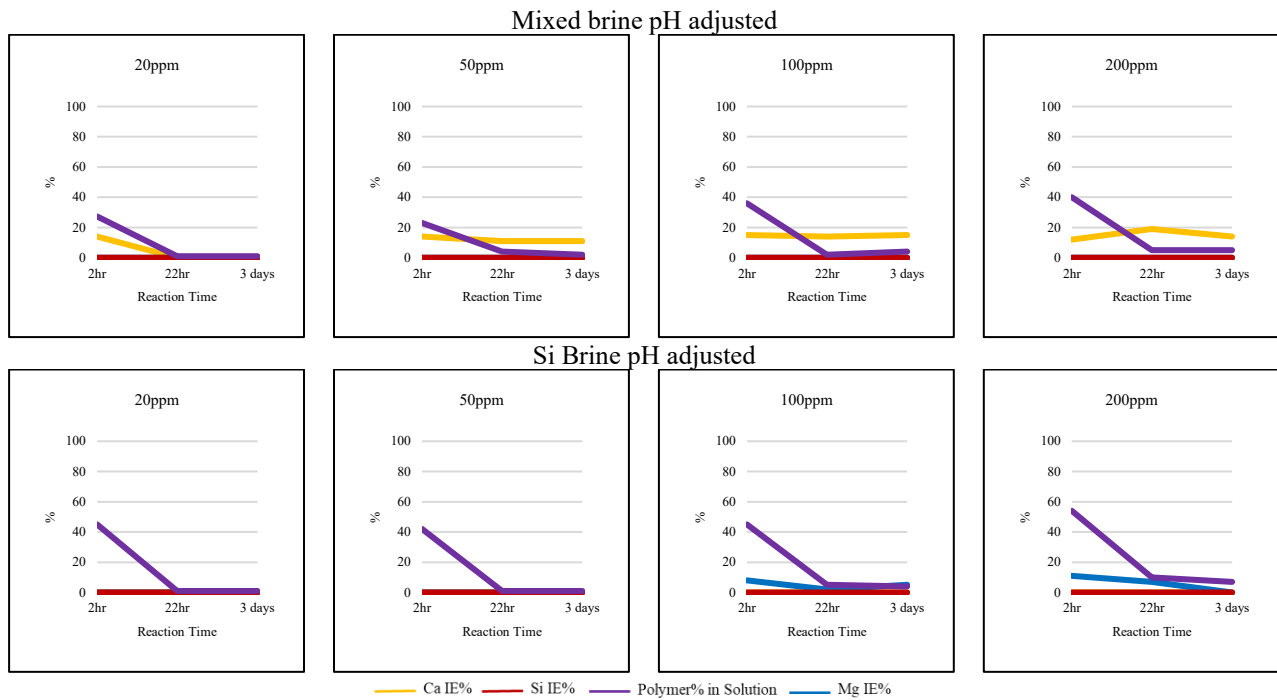


Fig. 7: SI B IE% and Polymer Consumption for 60Mg:940Si:500Ca at 95°C, pH8.5 and 20-200ppm SI B, Mixed Brine pH Adjusted vs. Silicon Brine pH Adjusted.

3.3 A5 Inhibition Efficiency and Mechanism for Silicate System of 60Mg:940Si at 95°C, pH8.5 and 20-200ppm SI Active Concentration

The ions reacted (%) are presented in Fig. 8. Plotted data shows that at pH8.5, more than 80% of magnesium and silicon ions were found to react in the blank solution at 2hrs reaction time and this trend remained constant over the 3 days reaction time. Having 100-200ppm A5 present, prevented the ions from reacting by decreasing the amount of Si and Mg ions reacted to less than 40% reaction. By raising the concentration of A5 from 100ppm to 200ppm, no further significant improvement was observed against inhibiting the silicate and magnesium scale.

The amorphous silicate and magnesium silicate inhibition efficiencies are shown in Fig. 9. A5 shows no inhibition efficiency at 20ppm and 50ppm with Si IE and Mg IE at zero % for 2hrs, 22hrs and 3 days. At 100ppm and 200ppm concentrations, a Si IE around 80-90% was observed over the 3 days reaction time. However, it appears that A5 cannot control magnesium silicate scale to an acceptable level, even when its concentration is increased to 100ppm or 200ppm, as it shows lower inhibition efficiency performance, ~60-70%.

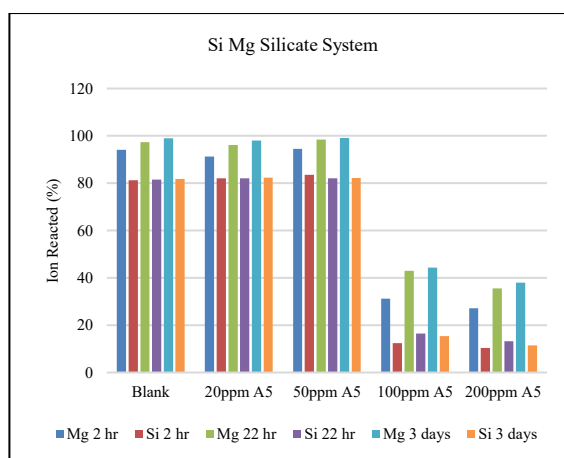


Fig. 8: Ion Reacted (%) for 60Mg:940Si at 95°C, pH8.5 and 20-200ppm A5.

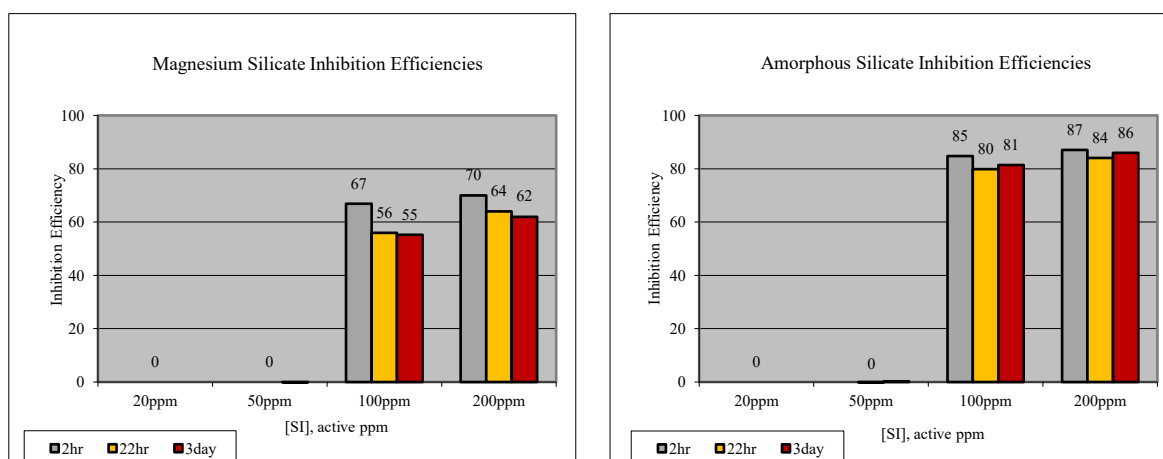


Fig. 9: Si and Mg IE% for 60Mg:940Si at 95°C, pH8.5 and 20-200ppm A5.

A series of experiments to monitor the level of A5 in solution at various times during the inhibition efficiency tests were performed. As the Hyamine technique was selected as being the more robust method for determining the consumption of scale inhibitor, the A5 inhibitor consumption results obtained from polymer analysis by Hyamine and Mg and Si IE% are shown in Fig. 10. At 200ppm A5, the corresponding polymer analysis shows a decline to 20-25%. At 100ppm, this decline is ~40-50%.

Similar to what was concluded for SI B in silicate system containing Si and Mg, when A5 sustains an efficiency of ~60% against magnesium silicate and ~60-80% against amorphous silicate, a smaller initial drop in its level is observed over 2hrs reaction time. Once crystallization begins, it effectively retarding crystals growth.

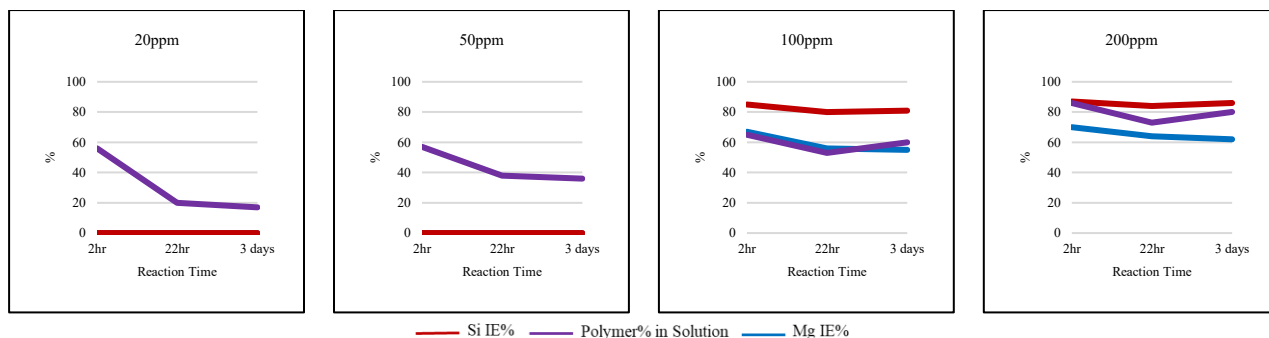


Fig. 10: A5 IE% and Polymer Consumption for 60Mg:940Si at 95°C, pH8.5 and 20-200ppm A5.

3.4 A5 Inhibition Efficiency and Mechanism for Silicate System of 60Mg:940Si:500Ca at 95°C, pH8.5 and 200ppm SI Active Concentration

Due to poor inhibition performance of SI B, only 200ppm trialed for A5 in the system containing Ca until data found to be useful. For this purpose, some sets of tests were designed and performed. When the pH of the mixed brine was adjusted to 8.5, approximately 10% of Ca ions reacted in the non-inhibited and 200ppm A5 solutions across all time intervals. In contrast, the percentage of Mg ions reacted increased from 80% to over 95% over time. The reaction of Si ions remained steady at around 80% over time across all samples. These results clearly indicate that the addition of 200ppm A5 to the system did not effectively control scale precipitation. It is worth mentioning that nothing special happened in the system when the pH of silicon brine was adjusted initially to 8.5 before mixing brines. When this pH adjusting method was taken, a considerable change occurred in the level of Mg ions reacted. Similar to what was observed for SI B, there was a drop of ~20% in the reacted Mg ions level at all time intervals for all sample solutions. However, Ca and Si ions showed the same amount of reaction and were not affected by this method of brine pH-adjusting.

The calculated Si, Ca and Mg inhibition efficiencies at 2hrs, 22hrs and 3 days indicate that 200ppm A5 is fully inefficient at preventing silicate-based scales. Mostly, this is due to presence of Ca ion in the system. In the lack of Ca ion, this system showed MIC ~100ppm A5 to prevent amorphous and magnesium silicate scale. Although A5 shows poor inhibition performance, the polymer depletion was ~60% over time. This trend was almost the same for both taken pH approaches. For this system with SI B (Fig. 7), the reduction in the scale inhibitor level was much more considerable, almost twice if it is compared to that for A5. This may be attributed to the presence of sulphonate groups in these scale inhibitors' molecular structure (Shaw et al., 2012). A developed ICP-OES analytical method was used to determine the sulphur content in SI B and A5, which was found to be approximately 2-2.5% and 4-5%, respectively. Sulphonate groups are highly ionic and remain largely dissociated in solution, meaning they do not form strong bonds with divalent metal ions such as Ca^{2+} and Mg^{2+} . Since SI B contains a lower concentration of sulphonate groups, it appears that higher Ca^{2+} and Mg^{2+} ions participate in bonding with it.

To assess whether the calcium present in the brine renders SI B and A5 completely ineffective, additional experiments were conducted. The results confirm that, as expected, the presence of calcium ions in the silicate system causes both A5 and SI B to lose their ability to prevent scale formation. A likely explanation is that calcium forms complexes with the polymeric functional groups of SI B and

A5, promoting polymer cross-linking and altering surface charge, ultimately leading to inhibition failure.

4. CONCLUSIONS

A static bottle test methodology was developed to assist in identification of efficient silicate inhibitors (IE% ~80-90%), applicable in low-enthalpy geothermal systems. To identify effective products for the control of silicate scaling, the inhibition mechanism and inhibition efficiency (IE) of two sulphonated polymer-based scale inhibitors, denoted A5 and SI B, were studied. This was performed for a brine containing $[Mg]_{\text{initial}} = 120\text{ppm}$ and $[Si]_{\text{initial}} = 1880\text{ ppm}$ at 95°C , pH 8.5 and SI active concentration range 20-200ppm. Further research was done to assess the impact of addition of $[Ca] = 500\text{ppm}$ to the non-inhibited and inhibited silicate system. Two methods were applied to assess the inhibition mechanism of SIs, one by measuring the concentration of sulphur (S) contained within their structure, by ICP-OES, and the other by using a matrix-matching Hyamine technique, to enable them to be assayed as a polymer product.

The outcomes of the research are as per following:

- MIC of ~50ppm SI B and ~100ppm A5 give IE performance at 70-90% with 40-60% polymer left in solution. Possibly, both SI B and A5, initially, show crystal growth blocking mechanism which means they inhibit better at long residence times after an initial drop in scale inhibitor concentration.
- When Ca is present, although two approaches were used to adjust the pH of the brine at 8.5 to reduce the tendency for $\text{Ca}(\text{OH})_2$ precipitation, and thereby improving scale inhibitor effectiveness, neither SI B nor A5 prevented precipitation of silicate-based scale.
- In the presence of Ca, despite SI B and A5 inefficiency, significant reduction in polymer level recorded. For SI B, the values detected for polymer were approximately zero after 3 days. For A5, this decrease was half, at 40-60%. This trend may be attributed to SI entrapment within the scale structure, where it becomes incorporated into the scale matrix without effectively blocking active growth sites on the crystal surface. Although they are consumed during the process, it is ultimately immobilized within the scale and fails to inhibit the precipitation of silicate-based scale effectively.
- To confirm whether calcium is responsible for the inefficiency of A5 and SI B, further research was conducted. Obtained results confirm that the Ca ion is the reason for A5 and SI B inefficiency at controlling silicate scaling. Possible suggestion is that Ca forms complexes with the SI B/A5 polymeric functional groups, leading to polymer cross-linking and surface charge changes that inactivate the SIs.

SOURCES

- Abib, G. A., Cruz, G. F. D., & VAZ, A. S.: Study of barium sulfate dissolution by scale dissolver based on solutions of DTPA, *Anais da Academia Brasileira de Ciências*, 90(3), (2018), 3185–3196.
- Amjad, Z., & Zuhl, R.: The role of water chemistry on preventing silica fouling in industrial water systems, *NACE CORROSION*, (2010).

- Anderson, R., Mozaffar, H., & Kalorazi, B. T.: Development of a crystal growth inhibition based method for the evaluation of kinetic hydrate inhibitors, *7th International Conference on Gas Hydrates*, (2011).
- Buscarlet, E., Richardson, I., Addison, S., Moon, H., Quinao, J., & Zealand, N.: Geochemical Modelling of Plant and Reservoir Processes at the Ngatamariki Geothermal Field, *38th New Zealand Geothermal Workshop*, (2016).
- Çiftçi, C., Karaburun, E., Tonkul, S., Baba, A., Demir, M. M., & Yeşilnacar, M. İ.: Testing the Performance of Various Polymeric Antiscalants for Mitigation of Sb-Rich Precipitates Mimicking Stibnite-Based Geothermal Deposits, *Geofluids*, 2020(1), (2020), 8867084.
- Finster, M., Clark, C., Schroeder, J., & Martino, L.: Geothermal produced fluids: Characteristics, treatment technologies, and management options, *Renewable and Sustainable Energy Reviews*, 50, (2015), 952–966.
- Gill, J. S.: New Inhibitors for silica and calcium carbonate control in geothermal, *International Workshop on Mineral Scaling*, (2011).
- Gören, A. Y., Topcu, G., Demir, M. M., & Baba, A.: Effect of high salinity and temperature on water–volcanic rock interaction, *Environmental Earth Sciences*, 80(3), (2021), 74.
- Graham, G. M., Boak, L. S., & Sorbie, K. S.: The influence of formation calcium and magnesium on the effectiveness of generically different barium sulphate oilfield scale inhibitors, *SPE production & facilities*, 18(01), (2003), 28–44.
- Haklıdır, F. T., & Haklıdır, M.: Fuzzy control of calcium carbonate and silica scales in geothermal systems, *Geothermics*, 70, (2017), 230–238.
- Hassani, K., & Zheng, W.: Mineral precipitation assessment of potential geothermal fluids in Clarke Lake field for future geothermal utilization, *Proceedings of Geoconvention Conference*, (2024).
- Hassani, K., & Zheng, W.: A review of recent advances in mineral scaling in geothermal energy systems: mechanisms, mitigation, and case studies, *Environmental Earth Sciences*, 84(14), (2025), 1–23.
- Hauksson, T., Pórhallsson, S., Gunnlaugsson, E., & Albertsson, A.: Control of magnesium silicate scaling in district heating systems, *World Geothermal Congress*, (1995).
- Heřmanská, M., Kleine, B. I., & Stefánsson, A.: Supercritical fluid geochemistry in geothermal systems, *Geofluids*, 2019(1), (2019), 6023534.
- Isik, T., Baba, A., Chandrasekharam, D., & Demir, M. M.: A brief overview on geothermal scaling, *Bulletin of the Mineral Research and Exploration*, 171(171), (2023), 185–203.
- Jarrhian, K., Mackay, E., Singleton, M., Mohammadi, S., Heath, S. M., & Pessu, F.: Scale Control in Geothermal Wells—What Are the Options for Effective and Economic Scale Management?, *SPE Journal*, 30(04), (2025), 2171–2189.
- Khasani, Deendarlianto, & Itoi, R.: Numerical study of the effects of CO₂ gas in geothermal water on the fluid-flow characteristics in production wells, *Engineering applications of computational fluid mechanics*, 15(1), (2021), 111–129.
- Khormali, A., Koochi, M. R., Varfolomeev, M. A., & Ahmadi, S.: Experimental study of the low salinity water injection process in the presence of scale inhibitor and various nanoparticles, *Journal of Petroleum Exploration and Production Technology*, 13(3), (2023), 903–916.
- Li, Y., Chen, Y., Peng, T., Qiao, S., Li, J., Liu, L., Liu, X., & Zheng, T.: An efficient silica scale inhibiting strategy for geothermal systems: Combination of cationic and anionic polymers, *Journal of Applied Polymer Science*, 140(32), (2023), 54245.
- Liu, Y., Dai, Z., Kan, A. T., Tomson, M. B., & Zhang, P.: Investigation of sorptive interaction between phosphonate inhibitor and barium sulfate for oilfield scale control, *Journal of Petroleum Science and Engineering*, 208, (2022), 109425.
- Matoorian, R., & Malaieri, M.: Flow Assurance Management in Geothermal Production Wells, *SPE Thermal Well Integrity and Production Symposium*, (2022).
- Morita, M., Yamaguchi, A., Koyama, S., & Motoda, S.: Method for imitating magnesium silicate scale formed at the geothermal power plant in Obama Hot Spring, Japan, *Geothermics*, 96, (2021), 102203.
- Mpelwa, M., & Tang, S.F.: State of the art of synthetic threshold scale inhibitors for mineral scaling in the petroleum industry: a review, *Petroleum Science*, 16(4), (2019), 830–849.
- Olajire, A. A.: A review of oilfield scale management technology for oil and gas production, *Journal of Petroleum Science and Engineering*, 135, (2015), 723–737.
- Ouerghi, F. H., Omri, M., Nisar, K. S., Abd El-Aziz, R. M., & Taloba, A. I.: Investigating the potential of geothermal energy as a sustainable replacement for fossil fuels in commercial buildings, *Alexandria Engineering Journal*, 97, (2024), 215–229.
- Pambudi, N. A., Itoi, R., Yamashiro, R., Alam, B. Y. C. S., Tusara, L., Jalilinasrabad, S., & Khasani, J.: The behavior of silica in geothermal brine from Dieng geothermal power plant, Indonesia, *Geothermics*, 54, (2015), 109–114.
- Petkowski, J. J., Bains, W., & Seager, S.: On the potential of silicon as a building block for life, *Life*, 10(6), (2020), 84.
- Scott, S., Galeczka, I. M., Gunnarsson, I., Arnorsson, S., & Stefánsson, A.: Silica polymerization and nanocolloid nucleation and growth kinetics in aqueous solutions, *Geochimica et Cosmochimica Acta*, 371, (2024), 78–94.

- Shah, M., Prajapati, M., Yadav, K., & Sircar, A.: A comprehensive review of geothermal energy storage: Methods and applications, *Journal of Energy Storage*, 98, (2024), 113019.
- Shaw, S. S., Sorbie, K. S., & Boak, L. S.: The Effects of Barium Sulfate Saturation Ratio, Calcium, and Magnesium on the Inhibition Efficiency—Part II: Polymeric Scale Inhibitors, *SPE Production & Operations*, 27(04), (2012), 390–403.
- Shi, Y., Li, Z., Li, Z., Chen, S., Yang, X., Duan, L., & Cai, J.: Synthesis and evaluation of scale inhibitor with high-temperature resistance and low corrosion capability for geothermal exploitation, *Journal of Petroleum Science and Engineering*, 218, (2022), 110976.
- Solano-Olivares, K., Santoyo, E., & Santoyo-Castelazo, E.: Integrated sustainability assessment framework for geothermal energy technologies: A literature review and a new proposal of sustainability indicators for Mexico, *Renewable and Sustainable Energy Reviews*, 192, (2024), 114231.